The Interplay Between Lattice Topology, Frustration, and Spin Quantum Number in Quantum Antiferromagnets on Archimedean Lattices

D. J. J. Farnell

School of Dentistry, Cardiff University,

Cardiff CF14 4XY, Wales, United Kingdom

O. Götze, J. Schulenburg, and R. Zinke

Institut für Theoretische Physik, Universität Magdeburg, D-39016 Magdeburg, Germany

R. F. Bishop and P. H. Y. Li

School of Physics and Astronomy, The University of Manchester,

Schuster Building, Manchester M13 9PL, United Kingdom

(Dated: November 3, 2018)

Abstract

The interplay between lattice topology, frustration, and spin quantum number, s, is explored for the Heisenberg antiferromagnet (HAFM) on the eleven two-dimensional Archimedean lattices (square, honeycomb, CaVO, SHD, SrCuBO, triangle, bounce, trellis, maple-leaf, star, and kagome). We show the CCM provides consistently accurate results when compared to the results of other approximate methods. The CCM also provides valuable information relating to the selection of ground states and we find that this depends on spin quantum number for the kagome and star lattices. Specifically, the $\sqrt{3} \times \sqrt{3}$ model state provides lower ground-state energies than those of the $q = 0$ model state for the kagome and star lattices for most values of s. The $q = 0$ model state provides lower ground-state energies only for $s = 1/2$ for the kagome lattice and $s = 1/2$ and $s = 1$ for the star lattice. The kagome and star lattices demonstrate the least amount of magnetic ordering and the unfrustrated lattices (square, honeycomb, SHD, and CaVO) demonstrate the most magnetic ordering for all values of s. The SrCuBO and triangular lattices also demonstrate high levels of magnetic ordering, while the remaining lattices (bounce, maple-leaf, and trellis) tend to lie between these extremes, again for all values of s. These results also clearly reflect the strong increase in magnetic order with increasing spin quantum number s for all lattices. The ground-state energy, $E_g/(NJs^2)$, scales with s^{-1} to first order, as expected from spin-wave theory, although the order parameter, M/s, scales with s^{-1} for most of the lattices only. Self-consistent spin-wave theory calculations indicated previously that M/s scales with $s^{-2/3}$ for the kagome lattice HAFM, whereas previous CCM results (replicated here also) suggested that M/s scales with $s^{-1/2}$. It is probable therefore that different scaling for M/s than with s^{-1} does indeed occur for the kagome lattice. By using similar arguments, we find here also that M/s scales with $s^{-1/3}$ on the star lattice and with $s^{-2/3}$ on the SrCuBO lattice.

Keywords: Archimedean Lattices; Heisenberg Antiferromagnets; High-Order Coupled Cluster Method (CCM)

I. INTRODUCTION

Archimedes was one of the first people to describe regular tilings in two spatial dimensions. Archimedean lattices [1–4] are infinite and they are composed of two-dimensional arrangements of regular polygons with every site equivalent. As shown in Fig. 1, there are eleven uniform two-dimensional Archimedean lattices. Such Archimedean "bodies" were gradually rediscovered in the Renaissance period by Piero della Fransceca, Luca Pacioli, Leonardo da Vinci, Albrecht Duerer, Daniele Barbaro, and Johannes Kepler [6]. Archimedean lattices are instantly appealing and they are seen in paintings and architecture. Indeed, these uniform Archimedean lattices are all around us: from patterns of household ceramic tiles, the weave in baskets ("kagomé" means "weave pattern" in Japanese), and on to the atomic structures of materials.

Quantum magnetic materials often demonstrate such regular patterns in the crystallographic structure of their magnetic atoms, which may interact via nearest-neighbour (NN) Heisenberg antiferromagnetic exchange interactions [2–4]. Even the more exotic Archimedean lattices have been realized, see, e.g., CaV_4O_9 (CaVO) [7], $SrCu_2(BO_3)_2$ (SrCuBO) [8], a polymeric iron(III) acetate (star) [9] or $Mx[Fe(O_2CCH_2)2NCH_2PO_3]_6nH_2O$ and $Cu_6Al(SO_4)(OH)_12Cl3H_2O$ (maple-leaf) [10]. Many of the Heisenberg antiferromagnets (HAFMs) on the Archimedean lattices are strongly "frustrated," where frustration occurs when bonds compete with each other. For the systems studied here, this is due to an intrinsic incompatibility between the exchange interaction and the underlying lattice geometry. Most of the Archimedean lattices contain triangles and are hence geometrically frustrated in the sense that not all pairs of NN spins can be simultaneously antiparallel, as is otherwise favored by the HAFM exchange interaction between pairs of spins. Indeed, the only unfrustrated cases here are for the square, honeycomb, SHD and CaVO lattices. Strong levels of such frustration can lead to novel states of quantum order or to states of magnetic disorder [5]. Such new physics that is driven by quantum mechanics is of immense interest to both theoreticians and experimentalists. Finally, the HAFM on the kagome lattice is of special importance in the field of quantum magnetism because it provides an example of novel topological state of matter [11–13], which might be realized by the material herbertsmithite [14]. The star lattice has much in common with the kagome lattice, including an infinitely degenerate ground state classically, although it has not been studied extensively. Although all sites on

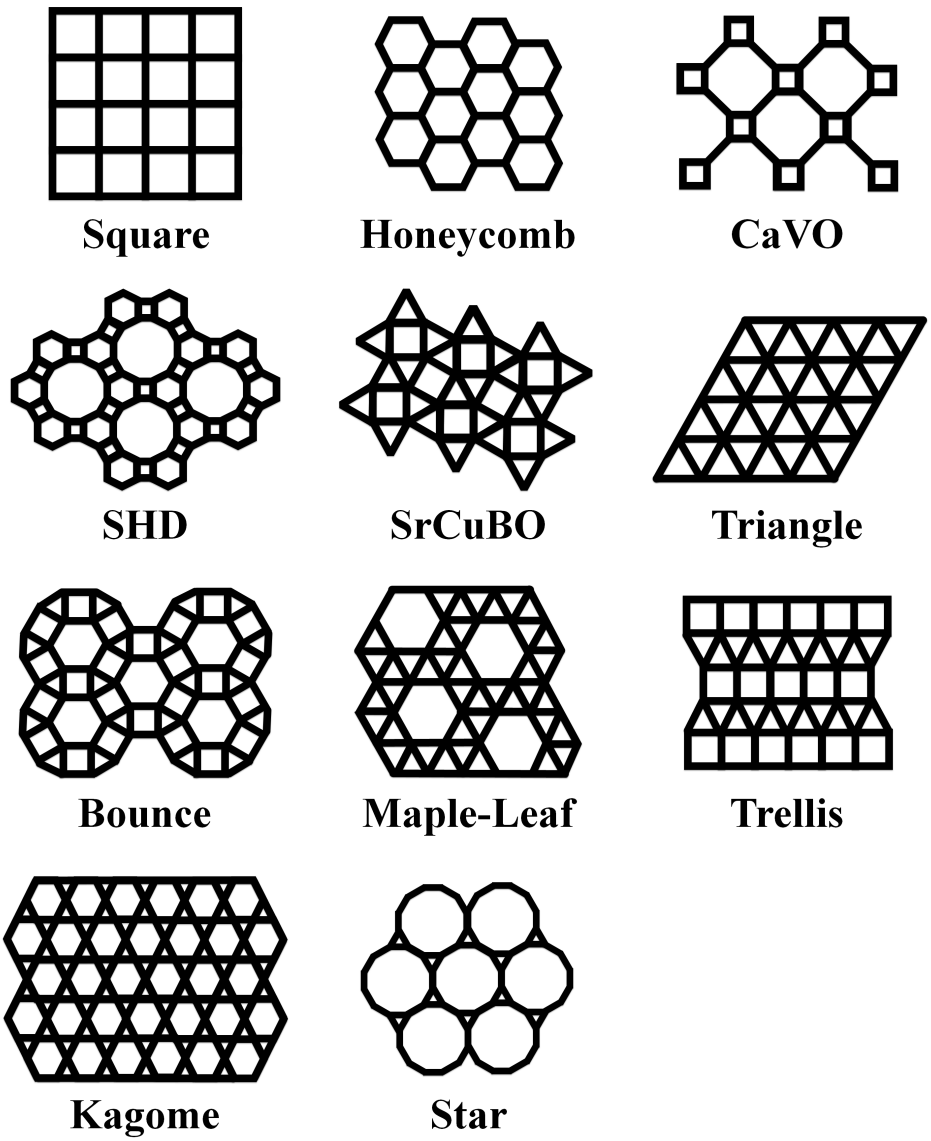

FIG. 1. The eleven Archimedean lattices: square (4^4), honeycomb (6^3), CaVO (4.8^2), SHD (4.6.12), SrCuBO ($3^2.4.3.4$), triangle (3^6), bounce (3.4.6.4), trellis ($3^3.4^2$), maple-leaf ($3^4.6$), star (3.12^2), and kagome (3.6.3.6). The mathematical description (in brackets) given by numbers n_i separated by dots (i.e., $n_1.n_2 \cdots n_r$) corresponds to the number of vertices of the polygons arranged around a vertex for each lattice.

the Archimedean lattices are equivalent, not all NN bonds on these lattices necessarily have to be equivalent for all lattices. For example, bonds on the CaVO lattice in Fig. 1 that lie on the squares are inequivalent to those bonds that connect these squares. This property gives us another criterion for dividing the Archimedean lattices into those lattices into which NN bonds are all equivalent (i.e., square, honeycomb, triangle, and kagome) and the rest of the lattices where not all NN bonds are equivalent. However, frustration is undoubtedly the stronger influence on the behavior of these systems.

Previous studies [1, 2] considered the properties of the Heisenberg antiferromagnet on the Archimedean lattices by using a method of quantum many-body theory called the coupled cluster method (CCM), although this was for the spin-half systems only. These analyses predicted (broadly) that three types of behavior occurs for the spin-half models: magnetically disordered systems (kagome and star); weakly ordered or possibly even disordered (maple-leaf, bounce, and trellis); and, magnetically ordered systems (square, honeycomb, CaVO, SHD, SrCuBO, and triangle). Here we obtain accurate results for the ground-state energy and the order parameter for all Archimedean lattices and for spin quantum numbers, $s \leq 4$. We provide results for scaling relations for both the ground-state energy and the order parameter as a function of the spin quantum number s, for each of the eleven lattices.

II. METHOD

The Hamiltonian of the HAFM is given by

$$H = J \sum_{\langle i,j \rangle} \mathbf{s}_i \cdot \mathbf{s}_j \quad , \tag{1}$$

where $\mathbf{s}$ is the spin operator on the lattice site i, $\mathbf{s}^2 = s(s+1)$, and $J > 0$. The symbol $\langle i, j \rangle$ indicates those bonds connecting adjacent sites (counting each bond once only). We consider this model here on all of the Archimedean lattices. The energy scale is set by putting $J = 1$ and the set of spin quantum numbers that we investigate here is $s \in \{\frac{1}{2}, 1, \frac{3}{2}, \cdots, 4\}$.

The coupled cluster method (CCM) [15–24] is one of the most powerful and most versatile modern techniques available to us in quantum many-body theory. It has previously been applied very successfully to various quantum magnetic systems. Details relating to the practical application of the CCM to these systems have been discussed extensively elsewhere (see e.g., [24–30]). We remark that the CCM performs well also for those systems that are

strongly frustrated. The main alternative approximate methods either cannot be applied or are sometimes of limited usefulness only in such cases. For example, QMC techniques may demonstrate the sign problem for such systems and the ED method is limited in practice by computational power, especially for $s > 1/2$, such that only very small lattices may be considered. Calculations for the density matrix renormalization (DMRG) method (and tensor-product methods) have generally been applied systems with lower spin quantum number as yet only in two spatial dimensions, although this method may also be applied in presence of strong frustration, in principle.

We present a brief overview of CCM formalism before going on to describe the some of the details only of the computational implementation of the CCM when it is applied to high-orders of approximation. Such computational methods are crucial to the accurate simulation of two-dimensional quantum magnetic systems. The highest level of approximation possible is limited only by the amount of computational resources available, as is described in an appendix for all of the Archimedean lattices and for spin quantum number $s \leq 4$. We begin any CCM calculation by choosing an appropriate *model* (or "*vacuum*") state that is denoted by $|\Phi\rangle$. The model state is the starting point for a CCM calculation and we build in any additional quantum effects with respect to this state. A complete set of basis states may be obtained by applying *creation* operators, $\{(C_L^+)\}$, to the model state. These creation operators are all mutually commuting. A detailed description of the possible choices of model state and associated choices of creation operators is given below for all of the Archimedean lattices. The corresponding Hermitian adjoints of $\{(C_L^+)\}$ are denoted by $\{(C_L)\}$. These sets of operators have the properties

$$\langle\Phi|C_L^+ = 0 = C_L|\Phi\rangle \quad \forall L \neq 0, \quad C_0^+ \equiv 1 \quad , \tag{2}$$

and

$$[C_L^+, C_J^+]_- = 0 = [C_L, C_J]_- \quad . \tag{3}$$

These operators are products of single-spin operators (see below) and so the index L indicates a set of single-spin indices simultaneously. For the set $\{|\Phi\rangle, C_L^+\}$ one defines that

$$\langle\Phi|C_L C_J^+|\Phi\rangle = \delta_{LJ} \quad , \tag{4}$$

and

$$\sum_L C_L^+|\Phi\rangle\langle\Phi|C_L = 1 = |\Phi\rangle\langle\Phi| + \sum_{L\neq 0} C_L^+|\Phi\rangle\langle\Phi|C_L \tag{5}$$

which correspond to orthonormality and completeness, respectively. Again, the operators C_L^+ act upon the model state $|\Phi\rangle$, which can be understood as a generalized vacuum state, and this approach allows for the construction of all possible states of the spin system. The CCM model states are often (though not always) given by the classical ground states of the lattice-spin systems under consideration. Thus, given a suitable model state and set of operators, $\{|\Phi\rangle, C_L^+\}$, the CCM parametrization of the exact ket and bra ground-state eigenvectors are given by

$$|\Psi\rangle = e^S|\Phi\rangle, \quad S = \sum_{L\neq 0} a_L C_L^+ \tag{6}$$

and

$$\langle\tilde{\Psi}| = \langle\Phi|\tilde{S}e^{-S}, \quad \tilde{S} = 1 + \sum_{L\neq 0} \tilde{a}_L C_L \quad , \tag{7}$$

for the ket and bra states, respectively. The operators S and $\tilde{S}$ are correlation operators for the ket and bra state, where $\{a_L\}$ and $\{\tilde{a}_L\}$ are the corresponding correlation coefficients. The summation includes all possible configurations of the system. Note that the following normalizations are fulfilled also:

$$\langle\Phi|\Psi\rangle = \langle\tilde{\Psi}|\Psi\rangle = \langle\Phi|\Phi\rangle = 1 \quad . \tag{8}$$

The ground-state energy equation is found by multiplying the Schrödinger equation $H|\Psi\rangle = E|\Psi\rangle$ (H is the Hamiltonian of the system) from the left with $\langle\Phi|e^{-S}$, and by using Eq. (6), to give

$$e \equiv \frac{E}{N} = \frac{1}{N}\langle\Phi|e^{-S}He^S|\Phi\rangle \quad . \tag{9}$$

The ground-state energy per spin e depends on the ket-state correlation coefficients $\{a_L\}$ only. Furthermore, the similarity transformation in Eq. (9) can be written as the usual nested commutator expansion,

$$e^{-S}He^S = H + [H,S]_- + \frac{1}{2}[[H,S]_-,S]_- + \cdots \quad . \tag{10}$$

Note also that this expression terminates after a finite set of terms if H contains only a finite number of single-spin operators, as here. The ket- and bra-state coefficients $\{a_L\}$ and $\{\tilde{a}_L\}$ can be determined by requiring that $\bar{H} = \langle\tilde{\Psi}|H|\Psi\rangle$ is stationary with respect to $\{\tilde{a}_L\}$ and $\{a_L\}$, respectively, which leads to the following equations

$$\frac{\partial\bar{H}}{\partial\tilde{a}_L} = 0 \Leftrightarrow \langle\Phi|C_L e^{-S}He^S|\Phi\rangle = 0, \forall L \neq 0, \tag{11}$$

and

$$\frac{\partial \bar{H}}{\partial a_L} = 0 \Leftrightarrow \langle \Phi | \tilde{S} e^{-S} [H, C_L^+]_- e^S | \Phi \rangle = 0, \forall L \neq 0 \quad . \tag{12}$$

The ground state is specified completely once the coefficients $\{a_L\}$ and $\{\tilde{a}_L\}$ have been found. Note that Eq. (11) is a nonlinear equation system in terms of the coefficients $\{a_L\}$ (ket equation system) and that Eq. (12) is a linear equation system in terms of the coefficients $\{\tilde{a}_L\}$ (bra equation system). For every observable, it follows therefore that

$$\bar{A} = \langle \tilde{\Psi} | A | \Psi \rangle = \bar{A}(\{a_L, \tilde{a}_L\}) \quad . \tag{13}$$

Here we use the order parameter M/s, which is defined by

$$\frac{M}{s} = -\frac{1}{sN} \sum_{i=1}^{N} \langle \tilde{\Psi} | \hat{s}_i^z | \Psi \rangle, \tag{14}$$

where we note that $\hat{s}_i^z$ is defined with respect to the local spin axes at site i (after rotation of the local spin axes) so that (notationally only) the spins in the model state appear to align in the negative z-direction (see also further below) at each site. If we set (trivially) all coefficients in S and $\tilde{S}$ to zero then the ground-state wave function $|\Psi\rangle$ is given by the model state $|\Phi\rangle$, and so the order parameter, M/s, is equal to 1 for all lattices in this classical limit. The effect of quantum fluctuations is to reduce to the amount of magnetic order and so we expect $M/s < 1$ for all lattices. (We expect that $M/s = 1$ is true only in the "classical" limit, i.e., $s \to \infty$.)

A discussion of the choice of model state for each lattice is given below, although we note again that a transformation of the local spin axes is used in all cases such that all spins point in the negative z-direction after "rotation." This process allows us to treat all spins equivalently and it simplifies the mathematical solution of the CCM problem considerably. The corresponding operators are used therefore with respect to the CCM model state, such that

$$|\Phi\rangle = \bigotimes_{i=1}^{N} |\downarrow\rangle_i, \;\; C_I^+ = s_{i_1}^+, s_{i_1}^+ s_{i_2}^+, s_{i_1}^+ s_{i_2}^+ s_{i_3}^+, \cdots \quad . \tag{15}$$

where i_1,i_2 and i_3 denote arbitrary lattice sites. The CCM formalism would be exact if all possible multi-spin cluster correlations could be included in S and $\tilde{S}$, although this is normally impossible to achieve practically. In most cases, the following approximation schemes within S and $\tilde{S}$ are used, namely:

- The SUBn scheme: all correlations involving only n or fewer spins are retained, although no further restriction is made concerning their spatial separation on the lattice;

- The SUBn-m scheme: all SUBn correlations spanning a range of no more than m adjacent lattice sites are retained; and

- The localized LSUBn scheme: all multi-spin correlations over all distinct locales on the lattice defined by n or fewer contiguous sites are retained.

Note that the LSUBn and SUBm-m schemes are identical for the limiting case when $s = 1/2$ and $n = m$. For higher spins s, the LSUBn scheme is equivalent to the SUBn-m scheme if and only if $n = 2 \cdot s \cdot m$. Note that we always use the SUBm-m scheme in this article. We see that these approximation schemes allow us to increase the level of approximation in a systemic and well-controlled manner. Furthermore, we can also attempt to extrapolate our "raw" SUBn, SUBn-m, and LSUBn results in the limits $n, m \to \infty$ in order to obtain even more accurate results. Although there is no general theory for the scaling behavior $m \to \infty$, there is nevertheless much empirical evidence relating to how to extrapolate the raw SUBm-m data [27–30]. For example, the following scheme is generally used for the ground-state energy per spin e,

$$e(m) = a_0 + a_1 m^{-2} + a_2 m^{-4} \quad . \tag{16}$$

By contrast, two commonly used extrapolation schemes for the order parameter M are given by

$$M_I(m) = b_0 + b_1 m^{-1} + b_2 m^{-2} \tag{17}$$

and

$$M_{II}(m) = c_0 + c_1 m^{-0.5} + c_2 m^{-1.5} \quad , \tag{18}$$

referred to as schemes I and II, respectively. Extrapolation scheme II is arguably more favorable for those systems that exhibit a magnetically disordered ground state and / or an order to disorder transition. The quality of the extrapolation is generally improved by omitting the lowest level of approximation, typically LSUB2 or SUB2-2, which is carried out only if enough data points for extrapolation are available. Furthermore, note that we extrapolate results for even values of m for the lattices: square, SHD, honeycomb, SrCuBO,

and CaVO. By contrast, we use both results from both odd and even values of m for all other lattices because the "odd/even" staggering effect [31] is much less pronounced for these frustrated systems, especially at higher orders of SUBm-m approximation.

The model states used here are the classical ground states (i.e., products of independent single-spin states) for all lattices. For example, the model state for all of the bipartite (unfrustrated) Archimedean lattices is the collinear (Néel) classical ground state in which nearest neighbor spins are antiparallel. The bipartite lattices are given by: square ($z = 4$) [27, 29, 30], honeycomb ($z = 3$) [32], CaVO ($z = 3$) [33], and SHD ($z = 3$) [1]. (z is the coordination number of the lattice.) The frustrated SrCuBO lattice ($z = 5$) uses a model state in which nearest-neighbor spins are antiparallel on the squares only for this lattice shown in Fig. 1. [34]. An explicit restriction is imposed on the creation operators $\{C_I^+\}$ in S for these model states, namely, that relationship $s_T^z = \sum_i s_i^z = 0$ in the original (unrotated) spin coordinates is preserved. This restriction guarantees that the approximate CCM ground-state wave function lies in the correct ($s_T^z = 0$) subspace for these lattices. The classical ground-state energy per bond for the HAFM on the square, honeycomb, CaVO, and SHD lattices is given by $-s^2$, whereas the classical ground-state energy per bond on the SrCuBO lattice is given by $-0.6s^2$. The model state for the triangular lattice ($z = 6$) [27] is given by spins on nearest-neighboring sites that form angles of 120° to each other. There is no restriction on s_T^z in this case and the classical ground-state energy per bond is given by $-0.5s^2$. The model states for the maple-leaf ($z = 5$) [35], trellis ($z = 5$) [1], and bounce ($z = 4$) [35] lattices are the classical ground states, and again there is no restriction on s_T^z. For both the maple-leaf and bounce lattices, the classical ground state comprises a six-sublattice struture with a specified pitch angle. By contrast, for the trellis lattice the classical ground state comprises incommensurate spirals along a chain direction. In all three cases, we take into account that quantum fluctuations can lead to a characteristic spiral or pitch angle that is different from its classical counterpart. Hence, in these three cases the characteristic angle is taken as a free parameter, which is selected in practice to minimize the respective ground-state energy obtained separately at level of SUBm-m level of approximation. The classical ground-state energy per bond is now given by $-s^2(1 + \sqrt{3})/5$ (maple-leaf) [35], $-0.65s^2$ (trellis) [2], and $-0.75s^2$ (bounce) [35]. Finally, the case for the kagome ($z = 4$) [36–38] and star ($z = 3$) [1, 2, 39] lattices is slightly more complicated because there are an infinite number of possible classical ground states to choose from potentially,

where each potential classical ground state has nearest-neighboring spins on the "triangles" of these lattices that form angles of 120° to each other. (The relative angles of those spins connecting triangles on the star lattice is 180°.) Here we consider the "$\sqrt{3}\times\sqrt{3}$" and "$q = 0$" states only. No restriction on s_T^z is imposed for either the kagome or star lattices and the classical ground-state energy per bond is given by $-0.5s^2$ and $-2s^2/3$ for the HAFM on the kagome and star lattices, respectively. The number of fundamental clusters that are distinct under the translational and point-group symmetries of the lattice and Hamiltonian (after rotation of local spin axes) and also that preserves s_T^z (as appropriate) is denoted $N_f = N_f(m)$ at a given level of SUBm-m approximation. The size of the CCM equations (measured in terms of the number of terms and also memory usage in bytes) at a given level of SUBm-m approximation is denoted $N_t = N_t(m)$.

CCM equations may be derived and solved analytically at low orders of approximation. A full explanation of how this is carried out for the SUB2-2 approximation for the spin-half XXZ model on the square lattice, for example, is given on pages 117 to 122 of Ref. [26]. However, highly intensive computational methods [27–30] rapidly become essential at higher orders of SUBm-m approximation because the number of fundamental clusters (and so therefore also the computational resources necessary to store and solve them) scales approximately exponentially with m. There are four distinct steps to carrying out high-order CCM calculations for the ground state and an efficient computer code has been developed [40]. The first step is to enumerate all (N_f) fundamental clusters that are distinct under the lattice and Hamiltonian symmetries (and perhaps that also satisfy $s_T^z = 0$) at a specific level of SUBm-m approximation and for a given lattice and spin quantum number s. The second step involves finding and storing the basic CCM ground- and excited-state equations. The third step involves solving both the ground- and excited-state equations and to obtain the macroscopic quantities for these states. A minimal ground-state energy solution as fnction of some explicit "angle" might be necessary if a "spiral" or "canted" model state [41] is used, as mentioned above. The fourth step is to create and input a basic script that defines completely the problem to be solved by the CCM code. Separate scripts were written for all eleven lattices considered here. The computational resources necessary to carry out high-order CCM calculations are considered in an Appendix.

III. RESULTS

Extrapolated results for the ground-state energy $E_g/(NJs^2)$ of the spin-half Heisenberg model on all of the lattices and for all values of spin quantum number, s, are given in Table I. Inspection of the extrapolated ground-state energy indicates that the $\sqrt{3} \times \sqrt{3}$ state is favored over the $q = 0$ state to form the ground state (i.e., it has lower ground-state energy) for the kagome and star lattices for most values of the spin quantum number, s. However, we find that the $q = 0$ state is favored over the $\sqrt{3} \times \sqrt{3}$ state for the kagome lattice for the specific case of $s = 1/2$ and it is favored over the $\sqrt{3} \times \sqrt{3}$ state for the star lattice for $s = 1/2$ and $s = 1$. As seen previously [1], CCM results for the ground-state energy per bond (in units of J) for the spin-half HAFM (i.e., $E_g/(JN_b)$: square, -0.3348; honeycomb, -0.3631; CaVO, -0.3689; SHD, -0.3702; SrCuBO, -0.2312; triangle, -0.1843; bounce, -0.2824; trellis, -0.2416; maple-leaf, -0.2124; star, -0.3110; kagome, -0.2179) compare well to those results of other approximate methods (i.e., $E_g/(JN_b)$: square, -0.3347 [42]; honeycomb, -0.3630 [43]; CaVO, -0.3691 [44]; SHD, -0.3688 [45]; SrCuBO, -0.23 to -0.24 [46]; triangle, -0.1823 [47]; bounce, -0.2837 [2]; trellis, -0.2471 [2, 39]; maple-leaf, -0.2171 [2]; star, -0.316 to -0.318 [48]; kagome, -0.21876 to -0.2193 [11–13, 49]). (N_b is the number of lattice bonds.)

Isolated results exist only for certain Archimedean lattices when we set $s > 1/2$. CCM results for the ground-state energy of the spin-one, square-lattice HAFM of $E_g/(NJs^2) = -2.32856$ compare well to results of second-order spin-wave theory [50] of -2.3284, third-order spin-wave theory [51] of -2.32815, and series expansions [50] of $-2.3279(3)$. CCM results for the ground-state energy of the spin-one, honeycomb-lattice HAFM of $E_g/(NJs^2) = -1.83061$ are in good agreement with results of spin-wave theory [53, 54] of -1.8313 and results of series expansions [54] of $-1.8278(8)$. CCM results for the ground-state energy for the spin-one, kagome-lattice HAFM of $E_g/(NJs^2) = -1.40315$ correspond well to results of Ref. [55] of $-1.410(2)$, Ref. [56] of $-1.4109(2)$, and Ref. [57] of -1.41095. CCM results for the ground-state energy for the $s = 3/2$, kagome-lattice HAFM of $E_g/(NJs^2) = -1.26798$ compare well to results of Ref. [58] of $-1.265(2)$. (Note that results for the scaling of the ground-state energy with spin quantum number s are also compared to results of spin-wave theory below, where they exist for the Archimedean lattices.)

Extrapolated results for the order parameter, M/s, for the HAFM on all of the lattices

and for all values of spin quantum number, s, are given in Table II. We see that the unfrustrated models (i.e.: square, honeycomb, SHD, and CaVO) and two frustrated lattices (i.e.: triangle and SrCuBO) are magnetically ordered for all values of the spin quantum number, s, including the limiting case of the spin-half systems. The HAFM on the trellis, bounce, and maple-leaf lattices is either disordered or very weakly magnetically ordered [1] for the spin-half system, and so results of both extrapolation schemes I and II of Eqs. (17) and (18) are given in Table II for $s = 1/2$ and for these lattices. By contrast, the HAFM is magnetically ordered for $s > 1/2$ for these lattices and so the extrapolation scheme I of Eq. (17) is used for $s > 1/2$. Results of both extrapolation schemes I and II of Eqs. (17) and (18) are given in Table II for the kagome and star lattices. Differences between the two extrapolation schemes I and II are seen in Table II for both the star lattice and (as noted previously in Ref. [38]) also for the kagome lattice. However, it is clear that the kagome and star lattices are predicted to be disordered (i.e., $M/s = 0$) by using both extrapolation schemes of Eqs. (17) and (18) for $s = 1/2$ [1]. By contrast, the kagome and star lattices are magnetically disordered (or weakly magnetically ordered) for $s = 1$. The kagome lattice is either weakly ordered or magnetically ordered for $s = 3/2$. Furthermore, it is clear also that all other results for higher s for the star ($s > 1$) and kagome ($s > 3/2$) lattices are magnetically ordered from both extrapolation schemes I and II.

As seen previously [1], CCM results for the order parameter M/s for the spin-half HAFM (i.e.: square, 0.619; honeycomb, 0.547; CaVO, 0.431; SHD, 0.366; SrCuBO, 0.404; triangle, 0.373; bounce, 0 to 0.122; trellis, 0.0 to 0.040; maple-leaf, 0 to 0.178; star, 0; kagome, 0) are again found to compare well to results of other approximate methods (i.e.: square, 0.614 [42]; honeycomb, 0.535 [59]; CaVO, 0.356 [60]; SHD, 0.509 [45]; SrCuBO, 0.42 [46]; triangle, 0.410 [61]; bounce, 0.268 [2]; trellis, 0.222 [2]; maple-leaf [2], 0.218; star, 0.094 to 0.15 [48]; kagome, 0 [11–13, 49]).

Again, isolated results exist only for the order parameter for certain Archimedean lattices with $s > 1/2$. CCM results for the order parameter of the spin-one, square-lattice HAFM of M/s =0.79942 compare well to spin-wave theory [50] of 0.8034, third-order spin-wave theory of [51] of 0.80427, and series expansions [50] of 0.8039(4), as well as recent results from infinite projected entangled pair states (iPEPS) [52] of M/s =0.802(7). CCM results for the order parameter of the spin-one, honeycomb-lattice HAFM of M/s =0.74123 are in good agreement with results of spin-wave theory of [53, 54] of M/s =0.7418 and results of series

expansions [54] of 0.748(3). Results of other approximate methods for the spin-one, kagome-lattice HAFM suggest that there is no magnetic long-range order [55–57, 62], although Ref. [63] indicated $\sqrt{3} \times \sqrt{3}$ ground-state long-range order for integer spin quantum numbers, including $s = 1$. Previous CCM calculations [64] for general spin quantum number concluded that CCM results were consistent with magnetic disorder for the spin-one, kagome-lattice HAFM. Series expansion calculations [62] indicated that $M/s = 0.14 \pm 0.03$ for the $s = 3/2$ kagome-lattice HAFM and recent tensor network calculations [58] also indicate that the $s = 3/2$ system is $\sqrt{3} \times \sqrt{3}$ long-range ordered. Indeed, the consensus from approximate methods [38, 63–65] is that the kagome-lattice HAFM demonstrates $\sqrt{3} \times \sqrt{3}$ ground-state long-range order for $s \geq 3/2$. (Note that results for the scaling of the order parameter with spin quantum number s are also compared to results of spin-wave theory below, where they exist for the Archimedean lattices.)

The scaling laws of the ground-state energy and the order parameter are shown in Table III and they are illustrated by Figs. 2 and 3, respectively. By allowing the index ν to vary as an explicit parameter for the ground-state energy in

$$\frac{E_g}{NJs^2} = \frac{E_{\rm cl}}{NJs^2} + \alpha s^{\nu} \quad , \tag{19}$$

we found that $E_g/(NJs^2)$ was found to scale with s^{-1} to leading order for all lattices. The classical result $E_{\rm cl}/(NJs^2)$ is known to be correct in the asymptotic limit $s \to \infty$ and so this expression is used explicitly in the scaling relations. As in Ref. [38], the extreme (quantum) cases of $s = 1/2$ and $s = 1$ are not used in fitting the data in Table I to the scaling relations (i.e., $s = \{3/2, 2, 5/2, 3, 7/2, 4\}$ are used here). The asymptotic relation for the ground-state energy to second order in s is therefore given by

$$\frac{E_g}{NJs^2} = \frac{E_{\rm cl}}{NJs^2} + \alpha s^{-1} + \beta s^{-2} \quad , \tag{20}$$

and the coefficients α and β are presented in this Table III for all lattices. Results for $E_g/(NJs^2)$ plotted as a function of s^{-1} are shown in Figs. 2. Associated line fits to the data using the values for α and β in Table III are shown also.

The index μ was allowed to vary as an explicit parameter for the order parameter in

$$\frac{M}{s} = 1 + \gamma s^{\mu} \quad . \tag{21}$$

Note that the classical result $M/s = 1$ in the limit $s \to \infty$ is assumed explicitly in this equation (as in Ref. [38]) and that the extreme (quantum) cases of $s = 1/2$ and $s = 1$ are

TABLE I. Extrapolated SUBm-m results for the ground-state energy $E_g/(NJs^2)$ for the HAFM on all Archimedean lattices and with $s \in \{1/2, 1, 3/2, \cdots, 4\}$. (The extrapolation scheme of Eq. (16) is used with (a) only even approximations with SUB4-4 or higher or (b) all data with SUB4-4 or higher. Results for the kagome and star lattices are shown for the $\sqrt{3} \times \sqrt{3}$ model state, except for $s = 1/2$ for the kagome lattice and $s = 1/2, 1$ for the star lattice where the results for the $q = 0$ state are shown.)

	$s = 1/2$	$s = 1$	$s = 3/2$	$s = 2$	$s = 5/2$	$s = 3$	$s = 7/2$	$s = 4$
Square$^{(a)}$	−2.67857	−2.32856	−2.21633	−2.16119	−2.12844	−2.10675	−2.09135	−2.07981
Honeycomb$^{(a)}$	−2.17885	−1.83061	−1.71721	−1.66159	−1.62862	−1.60681	−1.59133	−1.57976
CaVO$^{(a)}$	−2.21307	−1.84297	−1.72497	−1.66724	−1.63306	−1.61048	−1.59444	−1.58249
SHD$^{(a)}$	−2.22133	−1.84592	−1.72697	−1.66871	−1.63421	−1.61142	−1.59524	−1.58317
SrCuBO$^{(a)}$	−2.31212	−1.90314	−1.76867	−1.70159	−1.66135	−1.63452	−1.61535	−1.60097
Triangle$^{(b)}$	−2.21117	−1.84097	−1.72421	−1.66697	−1.63303	−1.61057	−1.59461	−1.58268
Bounce$^{(b)}$	−2.25904	−1.85797	−1.73423	−1.67405	−1.63845	−1.61493	−1.59823	−1.58578
Maple-Leaf$^{(b)}$	−2.12376	−1.72481	−1.60159	−1.54135	−1.50619	−1.48246	−1.46559	−1.45300
Trellis$^{(b)}$	−2.41580	−1.98823	−1.86186	−1.80073	−1.76467	−1.74142	−1.72447	−1.71183
Kagome$^{(b)}$	−1.74345	−1.40315	−1.26798	−1.20260	−1.16272	−1.13598	−1.11680	−1.10237
Star$^{(b)}$	−1.86622	−1.39597	−1.26002	−1.19494	−1.15595	−1.13002	−1.11152	−1.09766

not used in fitting the data to this scaling relation (i.e., $s = \{3/2, 2, 5/2, 3, 7/2, 4\}$ are used here). M/s was found to scale with s^{-1} to leading order for most lattices. However, it was found that M/s scales with $s^{-1/2}$ to first order for the kagome lattice (as seen previously in Ref. [38]), $s^{-1/3}$ to first order for the star lattice, and $s^{-2/3}$ to first order for the SrCuBO lattice. The results for the exponent of the star lattice are the least reliable here, which also shows the difficulty of simulating this system. For example, results for such line fits for the star lattice using data for $s = \{2, 5/2, 3, 7/2, 4\}$, $s = \{5/2, 3, 7/2, 4\}$, and $s = \{3, 7/2, 4\}$, respectively, suggest that the exponent for the order parameter might even have a magnitude that is less than 1/3. It is clear though that M/s does not scale with s^{-1} for the star lattice and that it is the most extreme case studied here. The asymptotic relation for the order

TABLE II. Extrapolated SUBm-m results for the order parameter M/s for the Heisenberg antiferromagnet on all Archimedean lattices and with $s \in \{1/2, 1, 3/2, \cdots, 4\}$. (The extrapolation scheme I of Eq. (17) is used with (c) only even approximations with SUB4-4 or higher or (d) all data with SUB4-4 or higher; (e) extrapolation scheme II of Eq. (18) is used with all data with SUB4-4 or higher. Results for the kagome and star lattices are shown for the $\sqrt{3} \times \sqrt{3}$ model state, except for $s = 1/2$ for the kagome lattice and $s = 1/2, 1$ for the star lattice where the results for the $q = 0$ state are shown.)

	$s = 1/2$	$s = 1$	$s = 3/2$	$s = 2$	$s = 5/2$	$s = 3$	$s = 7/2$	$s = 4$
Square$^{(c)}$	0.61862	0.79942	0.86634	0.90026	0.92053	0.93396	0.94340	0.95056
Honeycomb$^{(c)}$	0.54730	0.74123	0.82492	0.86894	0.89552	0.91319	0.92576	0.93514
CaVO$^{(c)}$	0.43058	0.70738	0.80302	0.85292	0.88297	0.90292	0.91708	0.92744
SHD$^{(c)}$	0.36647	0.68631	0.78847	0.84139	0.87356	0.89504	0.91033	0.92174
SrCuBO$^{(c)}$	0.40354	0.64239	0.72799	0.77385	0.80378	0.82563	0.84264	0.85642
Triangle$^{(d)}$	0.37251	0.68850	0.79845	0.85318	0.88487	0.90528	0.91946	0.92988
Bounce$^{(d)}$	0.12208 ($0^{(e)}$)	0.60091	0.73566	0.80221	0.84257	0.86956	0.88877	0.90310
Maple-leaf$^{(d)}$	0.17816 ($0^{(e)}$)	0.60681	0.73121	0.79685	0.82569	0.85387	0.87436	0.88988
Trellis$^{(d)}$	0.03980 ($0^{(e)}$)	0.61876	0.75301	0.81817	0.85670	0.87450	0.89304	0.90710
Kagome$^{(d)}$	0	0.15933	0.41742	0.49975	0.55729	0.59860	0.63018	0.65536
Kagome$^{(e)}$	0	0	0.07439	0.20290	0.29425	0.35825	0.40623	0.44397
Star$^{(d)}$	0	0.19158	0.42553	0.50031	0.54444	0.57197	0.58997	0.60233
Star$^{(e)}$	0	0	0.22317	0.35883	0.45135	0.51725	0.56665	0.60521

parameter M/s to second order with s is therefore given by

$$\frac{M}{s} = 1 + \gamma s^{-1} + \delta s^{-2} \quad , \tag{22}$$

for most lattices. (Appropriate relations to second order were used for the kagome, star and SrCuBO lattices, as described in Table III.) Results for γ and δ are shown in Table III. Results for M/s plotted as a function of s^{-1} are shown in Fig. 3. Associated line fits to the data using the values for γ and δ in Table III are shown also. For the sake of clarity, only

results for the order parameter obtained via extrapolation scheme I of Eq. (17) are included in Fig. 3 for the kagome and star lattices.

CCM results on the square lattice of $\alpha = -0.3161$ and $\gamma = -0.1961$ for the ground-state energy and order parameter, respectively, compare well to first order with results of spin-wave theory (SWT) [51] of $\alpha = -0.315895$ and $\gamma = -0.1966019$. CCM results on the honeycomb lattice of $\alpha = -0.3151$ and $\gamma = -0.2583$ for the ground-state energy and order parameter, respectively, also compare generally well to first order with results of SWT [53] of $\alpha = -0.31476$ and $\gamma = -0.2582$, respectively. CCM results on the triangular lattice of $\alpha = -0.3272$ and -0.2666 for the ground-state energy and order parameter, respectively, yet again compare well to first order with results of SWT [47] of $\alpha = -0.32762$ and $\gamma = -0.261303$ (see also Ref. [66]). Scaling results for the honeycomb lattice agree well with previous CCM results [67], although higher orders of approximation have been achieved here. Results for the kagome lattice from self-consistent spin-wave theory [68] state that the order parameter scales with $s^{-2/3}$. CCM results for M/s for kagome lattice for the $q = 0$ model state were found previously [38] to scale with $s^{-2/3}$. CCM results for M/s for the star lattice for the $q = 0$ model state are also found to scale with $s^{-2/3}$. Note again that the $\sqrt{3} \times \sqrt{3}$ model state has lower energy than the $q = 0$ state for $s \geq 1$ for the kagome lattice and $s \geq 3/2$ for the star lattice. In accordance with previous work [38] we remember again that M/s for the $\sqrt{3} \times \sqrt{3}$ ground state scales with $s^{-1/2}$ for the kagome lattice, rather than $s^{-2/3}$ as for the $q = 0$ state. It is this form of scaling that is shown in in Table III and in Fig. 3 for the kagome lattice. No scaling information with s exists from other approximate methods for the CaVO, SHD, SrCuBO, maple-leaf, bounce, trellis, or star lattices, as far as we are aware.

IV. CONCLUSIONS

We have explored the interplay between lattice topology and spin quantum number s on the magnetic ordering of the HAFM on Archimedean lattices in this article. High-order CCM calculations were carried out for all eleven Archimedean lattices by using highly intensive computational resources implemented on a parallel computing platform. It was shown in an appendix that the number of fundamental CCM clusters for the SUBm-m approximation and the memory resources scale approximately exponentially with increasing

TABLE III. Scaling of the ground-state energy in Table I and the order parameter in Table II with respect to s. (Scaling for the ground-state energy uses the relation: $E_g/(NJs^2) = E_{\rm cl}/(NJs^2) + \alpha s^{-1} + \beta s^{-2}$. Scaling for the order parameter use the relations: scheme (1) uses $M/s = 1 + \gamma s^{-1} + \delta s^{-2}$; scheme (2) uses $M/s = 1 + \gamma s^{-2/3} + \delta s^{-4/3}$; scheme (3) uses $M/s = 1 + \gamma s^{-1/2} + \delta s^{-1}$; and scheme (4) uses $M/s = 1 + \gamma s^{-1/3} + \delta s^{-2/3}$. All fits of the data to these relations were carried out using $s \geq 1.5$ (i.e., $s = \{3/2, 2, 5/2, 3, 7/2, 4\}$ are used here. Results are shown for the two extrapolation schemes I (d) and II (e) in Table II for the kagome and star lattices.)

	$E_g/(NJs^2)$			M/s	
	$E_{\rm cl}/(NJs^2)$	α	β	γ	δ
Square	-2	-0.3161	-0.0126	$-0.1961^{(1)}$	$-0.0066^{(1)}$
Honeycomb	-1.5	-0.3151	-0.0162	$-0.2583^{(1)}$	$-0.0067^{(1)}$
CaVO	-1.5	-0.3254	-0.0181	$-0.2873^{(1)}$	$-0.0125^{(1)}$
SHD	-1.5	-0.3281	-0.0186	$-0.3123^{(1)}$	$-0.0080^{(1)}$
SrCuBO	-1.5	-0.4042	0.0018	$-0.3708^{(2)}$	$0.0186^{(2)}$
Triangle	-1.5	-0.3272	-0.0137	$-0.2666^{(1)}$	$-0.0536^{(1)}$
Bounce	-1.5	-0.3382	-0.0197	$-0.3857^{(1)}$	$-0.0171^{(1)}$
Maple-leaf	-1.36603	-0.3450	-0.0124	$-0.4679^{(1)}$	$0.1008^{(1)}$
Trellis	-1.625	-0.3421	-0.0195	$-0.3678^{(1)}$	$-0.0006^{(1)}$
Kagome	-1	-0.4140	0.0180	$-0.6507^{(3)(d)}$	$-0.0779^{(3)(d)}$
				$-1.0676^{(3)(e)}$	$-0.0810^{(3)(e)}$
Star	-1	-0.3903	0.0005	$-0.5293^{(4)(d)}$	$-0.1366^{(4)(d)}$
				$-1.0576^{(4)(e)}$	$-0.0980^{(4)(e)}$

level of approximation level, m. Despite this, we have shown that the CCM can provide accurate results for the HAFM in all eleven Archimedean lattice, firstly by considering the limiting case of $s = 1/2$. Excellent correspondence with those results of other approximate methods was observed for both the ground-state energy and order parameter for the HAFM on all eleven Archimedean lattices, where they exist for $s \leq 4$. Accurate values for the ground-state energy are useful both experimentally and theoretically, where for example

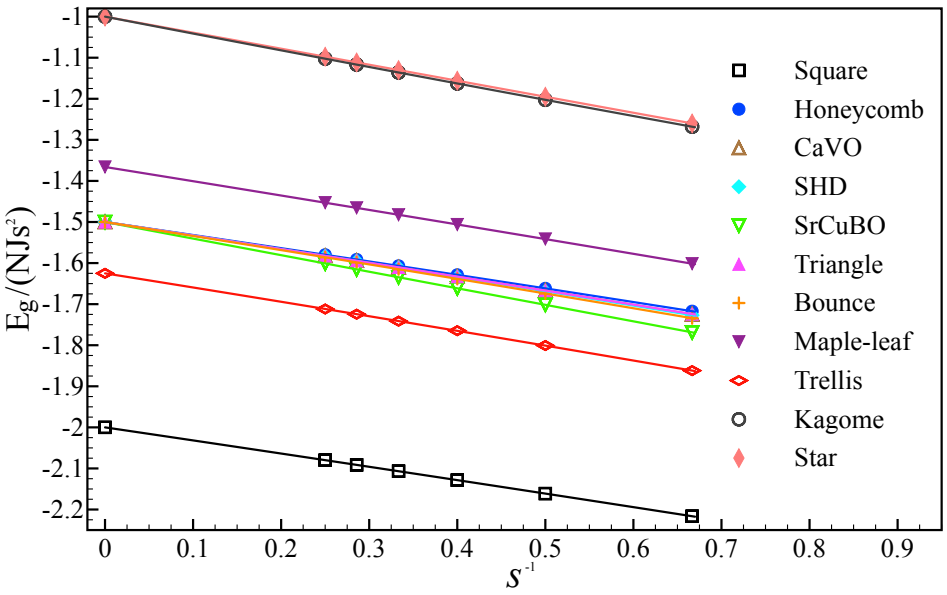

FIG. 2. (Color online) Results for the ground-state energy per site, $E_g/(NJs^2)$ plotted as a function of s^{-1} for $s \geq 3/2$. (Associated line fits to the data using the relations outlined in Table III are shown also.)

they are useful in thermodynamic studies at finite temperature [69–71]. See also Ref. [72] for a QMC treatment of the thermodynamic properties of the spin-one Heisenberg model on the square lattice and Ref. [73] for higher values of the spin quantum number. Ref. [74] details calculations using the Green function technique for the thermodynamics of the kagome-lattice Heisenberg antiferromagnet with arbitrary spin quantum number, and CCM results for the ground-state energy and the order parameter are more accurate than results presented in this paper. The ground-state energy and the order parameter are two fundamental parameters (among others) that define the behavior of quantum magnetic systems. Our results in Tables I and II therefore constitute an essentially quantitative reference for the Archimedean-lattice HAFMs with spin quantum number, $s \leq 4$.

Scaling relations for the ground-state energy and order parameter as a function of s were also presented for all of the Archimedean-lattice HAFMs. The scaling behavior for the ground-state energy was found to be the same as SWT, namely, that $E_g/(NJs^2)$ scaled with s^{-1} to first order. The scaling behavior for the order parameter was also found to be the

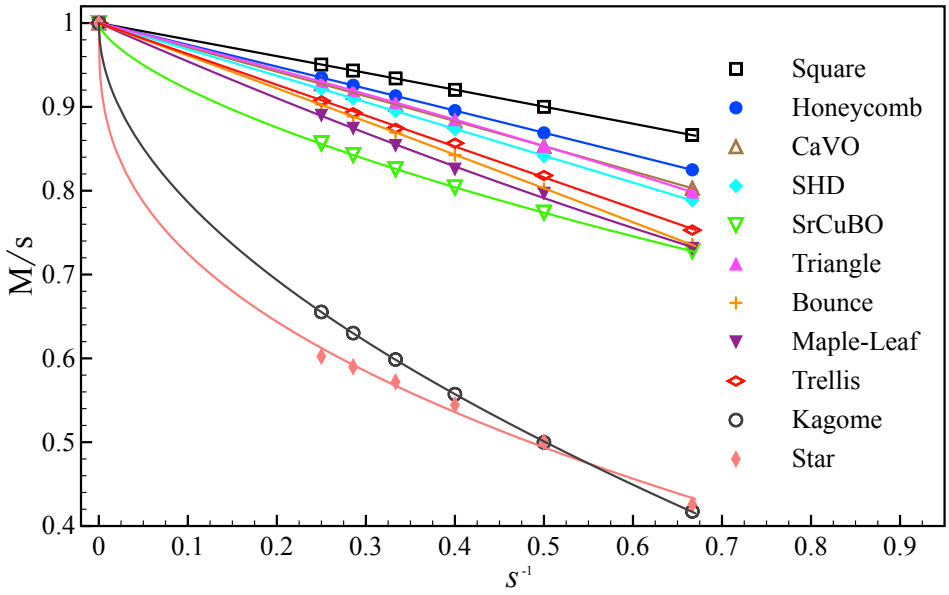

FIG. 3. (Color online) Results for the order parameter, M/s, plotted as a function of s^{-1} for $s \geq 3/2$. (Associated line fits to the data using the relations outlined in Table III are shown also. For the sake of clarity, results for the order parameter obtained via extrapolation scheme I of Eq. (17) are included here only for the kagome and star lattices for the $\sqrt{3} \times \sqrt{3}$ model state.)

same as that expected from linear SWT for most of the lattices, namely, that M/s scaled with s^{-1} to first order. Importantly, we remark again that self-consistent spin-wave theory calculations [68] showed that M/s scales with $s^{-2/3}$ for the kagome lattice HAFM, whereas previous CCM results [38] (found again here also) suggested that M/s scales with $s^{-1/2}$. We find also here that M/s scales with $s^{-1/3}$ on the star lattice and with $s^{-2/3}$ on the SrCuBO lattice. It would be interesting to see if self-consistent spin-wave theory might also detect this anomalous behavior for the star and SrCuBO lattices also, which has not been noticed before for these two lattices, as far as we are aware.

High-order SUBm-m calculations for large values of s suffer the double jeopardy of high computational demand and slow convergence with m. Thus, we assume the classical result $M/s \to 1$ in the limit $s \to \infty$ and we use CCM results for $s \leq 4$ only when evaluating the scaling behaviour. This is a limitation of these analyses, although it is particularly important only for the most extreme case of the star lattice. Despite this problem, expansion coefficients

for the ground-state and order parameter with s presented in Table III were found to compare well to first order to the results of other approximate methods, for those cases where they are known. Furthermore, CCM results for M/s for the kagome and star lattices for the $q = 0$ model state were found to scale with $s^{-2/3}$. These results give us confidence that anomalous scaling behavior to first order for the order parameter does indeed occur for the kagome, star, and SrCuBO lattices. The SrCUBO-lattice HAFM is a special case ($J_2 = 1$) of the Shastry-Sutherland antiferromagnet [75] that contains antiferromagnetic nearest-neighbor bonds J_1 on the square lattice and with one antiferromagnetic diagonal bond J_2 in each second square. It is known (e.g.) from Ref. [34] that a transition from Néel to plaquette order occurs at $J_2/J_1 = 1.477$ for the spin-half system. (Series expansions [76] place this point at $J_2/J_1 = 1.447$ and recent results of iPEPS [46] place it at $J_2/J_1 = 1.481$.) Furthermore, Néel order was found to disappear in the range $J_2/J_1 = 1.14$ to $J_2/J_1 = 1.39$ for this spin-half system in Ref. [34]. (Results of iPEPS [46] place this boundary at $J_2/J_1 = 1.307$.) The spin-half SrCuBO system might therefore be "close" (in some sense) to a disordered regime. However, it is still interesting and unexpected that the order parameter demonstrates such anomalous scaling with s for the SrCuBO-lattice HAFM. Both the star and kagome lattices have an infinite number of ground states classically, and so unusual behavior is perhaps less unexpected.

ACKNOWLEDGEMENT

We thank Prof. Johannes Richter for his insightful and interesting discussions relating to this work.

Appendix A: Computational Resources For High-Order CCM

We now wish to consider the computational resources that are necessary in order to carry out high-order CCM calculations for the Archimedean lattices for all values of the spin quantum number, s. Note that N_t is a measure of the number of terms and / or the memory usage of the CCM ket-state equation system; memory usage is a limiting factor of carrying out such large-scale CCM calculations. An additional complication for the bounce, trellis, and maple-leaf lattices is that we must carry out a dynamic search for the angle that

yields the lowest ground-state energy. Thus for example, SUB8-8 for $s < 3$ and SUB7-7 for $s \geq 3$ was achievable only for the trellis lattice. The highest SUBm-m level of approximation achieved by high-order CCM is shown in Table IV for all of the Archimedean lattices and for $s \in \{1/2, 1, 3/2, \cdots, 4\}$. The maple-leaf and bounce lattices both have large unit cells that contain six sites and so the number of fundamental clusters N_f increases strongly with increasing SUBm-m approximation level. Generally the computational effort [N_f, N_t] increases with the spin quantum number s and this is also shown in Table IV. For example, it was found previously [67] that $N_f = 103097$ for $s = 1/2$ at the SUB12-12 level of approximation on the honeycomb lattice, and $N_f = 538570$ for $s = 9/2$ at the SUB10-10 level of approximation for this lattice. Results for N_f and N_t (measured in terms of memory usage) on the square and kagome lattices and for $s = 1/2$ and $s = 4$ are plotted as a function of SUBm-m approximation level in Fig. 4. We see that the number of fundamental configurations and the memory usage both grow approximately exponentially with increasing level of SUBm-m approximation level (for a specific value of s). However, Table IV also shows that the number of fundamental configurations (and so also computer memory usage) saturates with increasing values of s for the SUBm-m scheme for a specific value of m. (Note that N_t refers to the number of terms contributing to the CCM equations rather than memory usage in this table, although clearly the two measures are linked.) The limiting factor here is the amount of computer resources available, thereby constraining the maximum value of m that is possible. Furthermore, the SUBm-m approximation constrains both the spatial separation of sites on the lattice (i.e., m contiguous sites) and also the maximum number of spin-flips (i.e., no more than m spin-flips). However, the maximum number of spin-flips per site is given by 2 for $s = 1$ systems generally, whereas the maximum number of spin-flips per site is given by 8 for $s = 4$ generally. It is the constraint on the maximum number of spin-flips for the SUBm-m approximation that leads to "saturation" with increasing s (keeping m constant). However, we remark that the SUB7-7 approximation (and certainly higher orders of approximation) ought to provide reasonable results for $s \lesssim 4$. By contrast, the LSUBn approximation does not restrict the number of spin-flips in any way and so we would not expect to observe a similar "saturation" with increasing s for this approximation scheme (keeping n constant). However, the LSUBn scheme is far more intensive in terms of computer resources than the SUBm-m scheme if we set $n = m$. Lower orders of LSUBn approximation scheme are possible only compared to the SUBm-m scheme, especially for

larger values of the spin quantum number. Note also that higher orders of approximation can be reached for some cases only via highly intensive computational methods that have been implemented for the CCM code using MPI. This approach "shares" out the cost (in terms of both the CPU time and memory usage) of finding and solving the CCM equations across all of processors that are used in parallel.

TABLE IV. The value of m for the highest level of SUBm-m approximation achieved by high-order CCM for the HAFM on all Archimedean lattices and with $s \in \{1/2, 1, 3/2, \cdots, 4\}$. The number of fundamental configurations and the number of terms in the ket-state equations at this highest level of SUBm-m approximation are shown also in square brackets (i.e., $[N_f, N_t]$). (N_t is presented in units of 10^{10} terms contributing to the CCM equations here.)

	$s = 1/2$	$s = 1$	$s = 3/2$	$s = 2$	$s = 5/2$	$s = 3$	$s = 7/2$	$s = 4$
Square	12 [766220, 1.89]	10 [1056286, 0.91]	10 [2006598, 1.55]	10 [2231647, 1.62]	10 [2253696, 1.66]	10 [2253696, 1.66]	9 [100011, 0.02]	9 [100011, 0.02]
Honeycomb	12 [103097, 0.10]	10 [219521, 0.11]	10 [461115, 0.20]	10 [530418, 0.21]	10 [538570, 0.22]	10 [538570, 0.22]	10 [538570, 0.22]	10 [538570, 0.22]
CaVO	12 [339887, 0.27]	10 [806870, 0.37]	10 [1744396, 0.72]	10 [2026614, 0.77]	10 [2061718, 0.79]	10 [2061718, 0.79]	10 [2061718, 0.79]	9 [126642, 0.79]
SHD	12 [241056, 0.18]	10 [607383, 0.28]	9 [93606, 0.01]	9 [98778, 0.01]	9 [98778, 0.01]	9 [98778, 0.01]	9 [98778, 0.01]	9 [98778, 0.01]
SrCuBO	10 [497361, 0.32]	8 [253957, 0.05]	8 [385889, 0.07]	8 [403292, 0.07]	8 [403292, 0.07]	8 [403292, 0.07]	8 [403292, 0.07]	8 [403292, 0.07]
Triangle	10 [1054841, 12.19]	8 [422399, 0.96]	8 [661675, 1.41]	8 [716945, 1.47]	8 [725541, 1.49]	8 [726350, 1.49]	8 [726386, 1.49]	8 [726387, 1.49]
Bounce	8 [182422, 0.14]	8 [1084987, 1.21]	8 [1850973, 1.94]	8 [2060029, 2.06]	8 [2099003, 2.1]	8 [2103493, 2.1]	8 [2103719, 2.11]	8 [2103721, 2.11]
Maple-Leaf	8 [110145, 0.11]	8 [1904330, 3.16]	8 [3158718, 4.90]	8 [3482740, 5.17]	7 [371833, 0.21]	7 [372037, 0.21]	7 [372039, 0.21]	7 [372039, 0.21]
Trellis	8 [80293, 0.10]	8 [1350826, 2.72]	8 [2189409, 4.10]	8 [2395909, 4.3]	8 [2430164, 4.36]	7 [242735, 0.17]	7 [242736, 0.17]	7 [242736, 0.17]
Kagome	10 [238010, 0.85]	8 [199717, 0.24]	8 [358075, 0.40]	8 [405130, 0.43]	8 [414668, 0.44]	8 [415871, 0.44]	8 [415934, 0.44]	8 [415935, 0.44]
Star	10 [28897, 0.03]	8 [45247, 0.02]	8 [89469, 0.05]	8 [105504, 0.05]	8 [109592, 0.05]	8 [110310, 0.05]	8 [110373, 0.05]	8 [110374, 0.05]

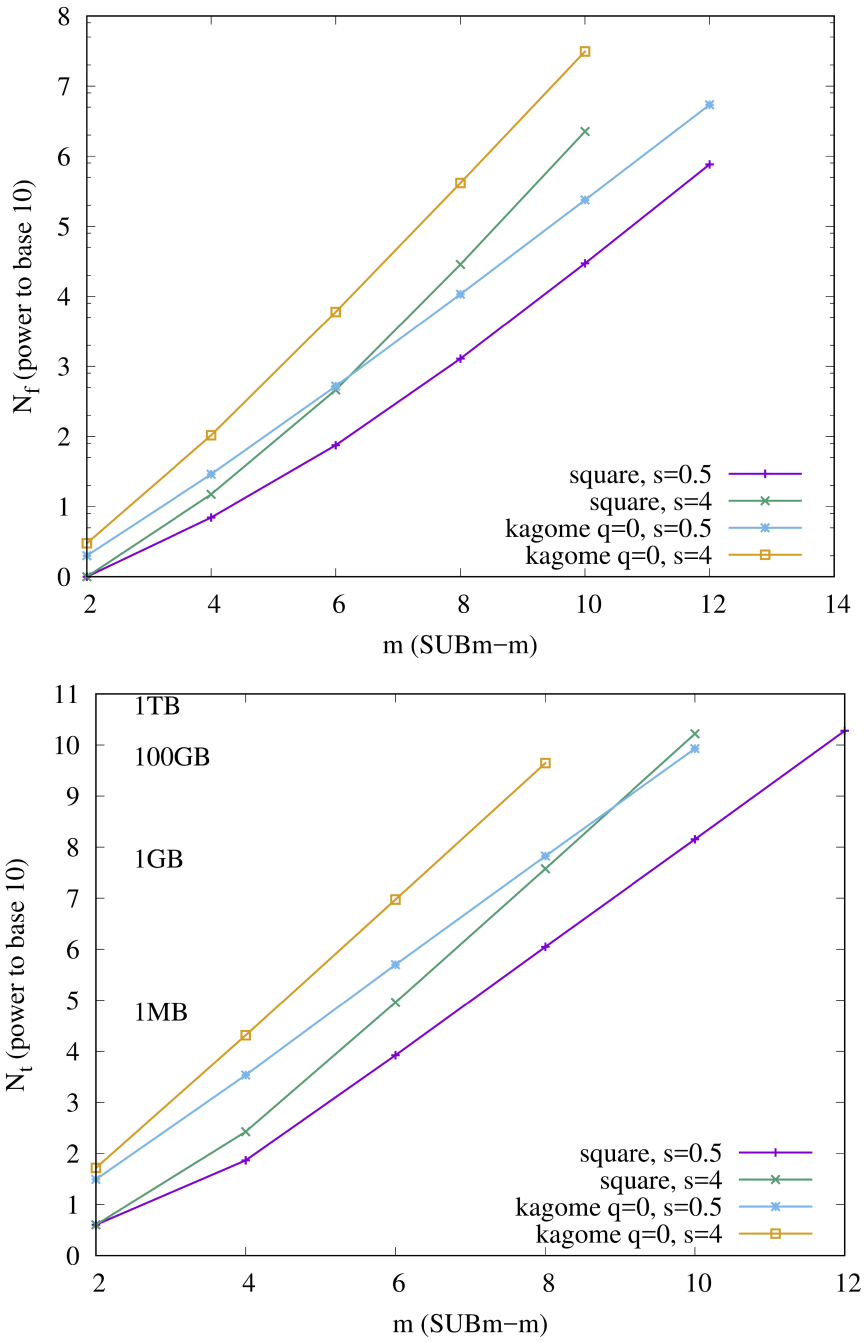

FIG. 4. (Color online) Illustration of the number of fundamental configurations N_f (top) and the number of terms N_t (measured in terms of memory usage here) of the ket equation system (bottom) plotted as a function of the approximation m. The square and the kagome lattices with $s = \frac{1}{2}$ and $s = 4$ have been chosen as examples. Note that the N_f and the N_t data are scaled logarithmically (base 10) and that the data for even numbers of m are shown only.

[1] D.J.J. Farnell, O. Götze, J. Richter, R.F. Bishop, and P.H.Y. Li, Phys. Rev. B **89**, 184407 (2014).

[2] J. Richter, J. Schulenburg, and A. Honecker, Lect. Notes Phys. **645**, 85-153 (Springer Berlin Heidelberg, 2004).

[3] Y. Unjong, Phys. Rev. E **91**, 062121 (2015).

[4] Y.Z. Zheng, Z. Zheng, and X.M. Chen, Coordination Chemistry Reviews **258-259**, 1 (2014).

[5] L. Balents, Nature **464**, 199 (2010).

[6] J.V. Field. Archive for the History of Exact Sciences **50**, 241-289 (1997).

[7] S. Taniguchi, T. Nishikawa, Y. Yasui, Y. Kobayashi, M. Sato, T. Nishioka, M. Kontani, and K. Sano, J. Phys. Soc. Jpn. **64**, 2758 (1995).

[8] H. Kageyama, K. Yoshimura, R. Stern, N. V. Mushnikov, K. Onizuka, M. Kato, K. Kosuge, C. P. Slichter, T. Goto, and Y. Ueda, Phys. Rev. Lett. **82**, 3168 (1999).

[9] F. Grandjean and G. J. Long, Angew. Chem. Int. Ed. **46**, 6076 (2007).

[10] T. Fennell, J.O. Piatek, R.A. Stephenson, G.J. Nilsen, and H.M. Ronnow, J. Phys.: Condens. Matter **23**, 164201 (2011).

[11] H. J. Liao, Z. Y. Xie, J. Chen, Z. Y. Liu, H. D. Xie, R. Z. Huang, B. Normand, and T. Xiang, Phys. Rev. Lett. **118**, 137202 (2017).

[12] S. Yan, D.A. Huse, and S.R. White, Science **332**, 1173 (2011).

[13] S. Depenbrock, I. P. McCulloch, and U. Schollwöck, Phys. Rev. Lett. **109**, 067201 (2012).

[14] P. Mendels, F. Bert, M.A. de Vries, A. Olariu, A. Harrison, F. Duc, J.C. Trombe, J.S. Lord, A. Amato, and C. Baines, Phys. Rev. Lett. **98**, 077204 (2007).

[15] F. Coester, Nucl. Phys. **7**, 421 (1958); F. Coester and H. Kümmel, *ibid.* **17**, 477 (1960).

[16] J. Čižek, J. Chem. Phys. **45**, 4256 (1966); Adv. Chem. Phys. **14**, 35 (1969).

[17] R.F. Bishop and K.H. Lührmann, Phys. Rev. B **17**, 3757 (1978); *ibid.* **26**, 5523 (1982).

[18] H. Kümmel, K.H. Lührmann, and J.G. Zabolitzky, Phys Rep. **36C**, 1 (1978).

[19] J.S. Arponen, Ann. Phys. (N.Y.) **151**, 311 (1983).

[20] R.F. Bishop and H. Kümmel, Phys. Today **40(3)**, 52 (1987).

[21] J.S. Arponen, R.F. Bishop, and E. Pajanne, Phys. Rev. A **36**, 2519 (1987); *ibid.* **36**, 2539 (1987); in: *Condensed Matter Theories*, Vol. **2**, P. Vashishta, R.K. Kalia, and R.F. Bishop,

eds. (Plenum, New York, 1987), p. 357.

[22] R.J. Bartlett, J. Phys. Chem. **93**, 1697 (1989).

[23] R.F. Bishop, Theor. Chim. Acta **80**, 95 (1991).

[24] R. F. Bishop, in *Microscopic Quantum Many-Body Theories and Their Applications*, edited by J. Navarro and A. Polls, Lecture Notes in Physics, Vol. 51 (Springer, Berlin, 1998), p.1.

[25] D. J. J. Farnell and R. F. Bishop, in *Quantum Magnetism*, edited by U. Schollwöck, J. Richter, D. J. J. Farnell, and R. F. Bishop, Lecture Notes in Physics, Vol. 645 (Springer, Berlin, 2004), p. 307.

[26] J. B. Parkinson and D. J. J. Farnell, Lect. Notes Phys. **816**, 109-134 (Springer Berlin Heidelberg, 2010). **816**.

[27] C. Zeng, D. J. J. Farnell, and R. F. Bishop, J. Stat. Phys. **90**, 327 (1998).

[28] D.J.J. Farnell, K.A. Gernoth, and R.F. Bishop, J. Stat. Phys. **108**, 401 (2002).

[29] R.F. Bishop, D.J.J. Farnell, S.E. Krüger, J.B. Parkinson, J. Richter, and C. Zeng, J. Phys.: Condens. Matter **12** 6887 (2000).

[30] R. Darradi, O. Derzhko, R. Zinke, J. Schulenburg, S. E. Krüger, and J. Richter, Phys. Rev. B **78**, 214415 (2008).

[31] D.J.J. Farnell and R. F. Bishop, Int. J. Mod. Phys. B **22**, 3369 (2008).

[32] D.J.J. Farnell, R. F. Bishop, P. H. Y. Li, J. Richter, and C. E. Campbell. Phys. Rev. B **84**, 012403 (2011).

[33] D.J.J. Farnell, J. Schulenberg, J. Richter, and K.A. Gernoth, Phys. Rev. B **72**, 172408 (2005).

[34] R. Darradi, J. Richter, and D.J.J. Farnell, Phys. Rev. B. **72**, 104425 (2005).

[35] D.J.J. Farnell, R. Darradi, R. Schmidt, and J. Richter. Phys. Rev. B **84**, 104406 (2011).

[36] D.J.J. Farnell, K.A. Gernoth, and R.F. Bishop, Phys. Rev. B **63**, R220402 (2001).

[37] R.F. Bishop, P.H.Y. Li, D.J.J. Farnell, and C.E. Campbell, Phys. Rev. B **82**, 104406 (2010).

[38] O. Götze, D.J.J. Farnell, R.F. Bishop, P.H.Y. Li, and J. Richter, Phys. Rev. B **84**, 224428 (2011).

[39] J. Richter, J. Schulenburg, A. Honecker and D. Schmalfuß, Phys. Rev. B **70**, 174454 (2004).

[40] http://www-e.uni-magdeburg.de/jschulen/ccm/index.html

[41] R. Zinke, S.-L. Drechsler, and J. Richter, Phys. Rev. B **79**, 094425 (2009).

[42] A.W. Sandvik, Phys. Rev. B **56**, 11678 (1997)

[43] J.D. Reger, J.A. Riera, and A.P. Young, J. Phys.: Condens. Matter **1**, 1855 (1989).

[44] A. Jagannathan, R. Moessner, and S. Wessel, Phys. Rev. B **74**, 184410 (2006).

[45] P. Tomczak, J. Schulenburg, J. Richter, and A.R. Ferchmin, J.Phys.: Condens. Matter **13**, 3851 (2001),

[46] P. Corboz and F. Mila, Phys. Rev. B **87**, 115144 (2013).

[47] A. L. Chernyshev and M. E. Zhitomirsky, Phys. Rev. B **79**, 144416 (2009).

[48] B.-J. Yang, A. Paramekanti, and Y. B. Kim, Phys. Rev. B **81**, 134418 (2010).

[49] A.M. Läuchli, J. Sudan, and E.S. Sørensen, Phys. Rev. B **83**, 212401 (2011).

[50] Zheng Weihong, J. Oitmaa, and C.J. Hamer, Phys. Rev. B **43**, 8321 (1991).

[51] C.J. Hamer, Zheng Weihong, and P. Arndt, Phys. Rev. B **46**, 6276 (1992).

[52] I. Niesen and P. Corboz, Phys. Rev. B **95**, 180404(R) (2017).

[53] Zheng Weihong, J. Oitmaa, and C.J. Hamer. Phys. Rev. B **44**, 11869 (1991).

[54] J. Oitmaa, C.S. Hamer, and Zheng Weihong, Phys. Rev. B **45**, 9834 (1992).

[55] H. Changlani and A.M. Läuchli., Phys. Rev. **B** 91, 100407(R) (2015)

[56] T. Liu, W. Li,A. Weichselbaum, J. von Delft, and G. Su, Phys. Rev. B **91**, 060403(R) (2015).

[57] S. Nishimoto and M. Nakamura, Phys. Rev. B **92**, 140412(R) (2015) .

[58] T. Liu, W. Li, and G. Su, Phys. Rev. E 94, 032114 (2016).

[59] E.V. Castro, N.M.R. Peres, K.S.D. Beach, and A.W. Sandvik, Phys. Rev. B **73**, 054422 (2006).

[60] M. Troyer, H. Kontani, and K. Ueda, Phys. Rev. Lett. **76**, 3822 (1996).

[61] S.R. White and A.L. Chernyshev, Phys. Rev. Lett. **99**, 127004 (2007).

[62] J. Oitmaa and R.R.P. Singh, Phys. Rev. B **93**, 014424 (2016).

[63] O. Cépas and A. Ralko, Phys. Rev. B **84**, 020413 (2011).

[64] O. G$\acute{}$otze and J. Richter, Phys. Rev. B **91**, 104402 (2015).

[65] A. L. Chernyshev and M. E. Zhitomirsky, Phys. Rev. Lett. **113**, 237202 (2014).

[66] A.V. Chubukov, S. Sachdev, and T. Senthil, J. Phys.: Condens. Matt. **6**, 8891 (1994).

[67] P.H.Y. Li, R.F. Bishop, and C.E. Campbell. J. Phys.: Conf. Ser. **702**, 012001 (2016).

[68] A. Chubukov, Phys. Rev. Lett. **69**, 832 (1992).

[69] B. Bernu and G. Misguich, Phys. Rev. B **63** 134409 (2001).

[70] G. Misguich and B. Bernu, Phys. Rev. B **71**, 014417 (2005).

[71] H.-J. Schmidt, A. Hauser, A. Lohmann, and J. Richter, Phys. Rev. E **95**, 042110 (2017).

[72] K. Harada M. Troyer, and N.Kawashima, J. Phys. Soc. Jpn. **67**, 1130 (1998).

[73] D. C. Johnston, R. J. McQueeney, B. Lake, A. Honecker, M. E. Zhitomirsky, R. Nath, Y. Furukawa, V. P. Antropov, and Yogesh Singh, Phys. Rev. B **84**, 094445 (2011).

[74] P. Müller, A. Zander, and J. Richter, Phys. Rev. B **98**, 024414 (2018).

[75] B. S. Shastry and B. Sutherland, Physica B+C **108**, 1069 (1981).

[76] Zheng Weihong, C. J. Hamer, and J. Oitmaa, Phys. Rev. B **60** 6608 (1999).